

# Surface grating loaded VCSEL with single mode power of over 80 mW

Shanting Hu<sup>1, 2, a)</sup>, Ahmed Hassan<sup>2, 3</sup>, Xiaodong Gu<sup>2, 4</sup>, Masanori Nakahama<sup>2, 4</sup>, and Fumio Koyama<sup>2</sup>

**Abstract** We demonstrate a surface grating loaded VCSEL showing high power, good beam quality and stable single mode operation. In the structure, a single slow light mode propagating laterally along the long cavity of an oxide VCSEL can be selected thanks to the surface Bragg-grating. Experimental results of spectrum, L/I characteristics and beam quality with different device lengths are presented. A single mode power of over 80 mW is realized with a narrow diffraction-limited divergence angle of 0.15° for a VCSEL with an oxide aperture of 4 μm × 500 μm under CW operation. A higher single mode power is expected through extending the device length with the proven scaling law.

**Keywords:** VCSELs, slow light, high power, single mode operation

**Classification:** Semiconductor lasers

## 1. Introduction

With various advantages such as low cost and low power consumptions, VCSEL has been a key light source in short-reach optical communication systems [1, 2, 3, 4, 5]. As technology matures, VCSEL applications diversified including laser mice, printers, medical imaging and so on [6, 7, 8, 9, 10, 11]. In recent years, VCSEL technology for 3D sensing has been attracting more and more interests [12, 13, 14, 15, 16]. For 3D sensing applications such as LiDAR, a high-power light source has been developed. At the current stage, a common solution is to utilize two-dimensional VCSEL arrays, which offer kW-class output powers [17, 18, 19]. However, external optical elements are needed for beam convergence since the beam divergence angle of the array is over 10°, which adds costs and complexities to the sensing system. Thus, a new VCSEL technology with high power and high beam quality emerges as a challenge for new applications.

In our group, we demonstrated the slow light VCSEL amplifier with single mode output power of over 8 W and a narrow diffraction-limited divergence beam below 0.03° [20, 21, 22]. An input light is coupled through a lensed fiber to a lateral propagation mode with a small group velocity so

called “slow light”. The slow light can be amplified along the long cavity with pumping the VCSEL amplifier above the threshold and is emitted from the top surface. In this case, the amplified output is proportional to the amplifier length and the beam divergence is getting smaller and smaller with increasing the length. Very recently we came to the idea to utilize either the surface grating structure or coupled cavity to select a single slow light mode of the long cavity VCSEL itself, which we call a “slow-light laser” [23, 24]. However, since high order grating is applied in the first demonstration, there still remains issues in achieving good mode stability in the entire current range.

In this paper, we present a slow light laser based on 1st-order surface grating loaded VCSEL exhibiting the stable single-mode operation in the entire current range and a single-mode power over 80 mW.

## 2. Device structure

The schematic structure of a surface grating loaded VCSEL is illustrated in Fig. 1 (a). The proposed slow-light VCSEL has the same vertical structure as the conventional oxide-confined VCSEL except that the top surface is periodically etched to form lateral Bragg-grating mirrors. Similar to a DFB edge emitting laser [25, 26, 27, 28], a single slow-light mode nearly at the Bragg-wavelength at a tilted angle can be selected due to the optical feedback in the grating. We expect various advantages in our new structures. No face damages cannot be seen, which could be one of limiting factors in high-power GaAlAs edge emitting lasers. The fabrication

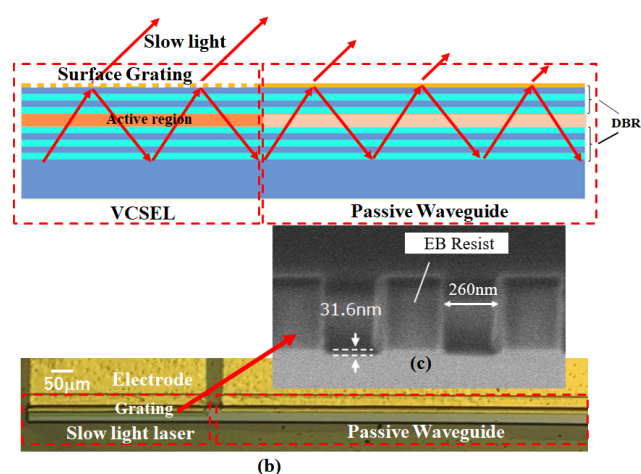


**Fig. 1** (a) Schematic side view of the proposed slow light laser; (b) top view of a fabricated device; (c) magnified cross-sectional view of the grating region

<sup>1</sup> Beijing University of Posts and Telecommunications, No.10 Xitucheng Road, Haidian District, Beijing, China

<sup>2</sup> Laboratory for Future Interdisciplinary Research of Science and Technology, Tokyo Institute of Technology, 4259 Nagatsuta, Midoriku, Yokohama 226–8503, Japan

<sup>3</sup> Department of Physics, Faculty of Science, Al-Azhar University, Assuit, Egypt

<sup>4</sup> Ambition Photonics Inc., Tokyo Tech Yokohama Venture Plaza E208, Yokohama 226–8510, Japan

<sup>a)</sup> hu.s.ab@m.titech.ac.jp

is the same as well-established conventional VCSELs except surface grating process. The phase index for slow-light modes is smaller than unity thanks to large waveguide dispersion [29]. The grating pitch of the 1st-order grating is typically 0.5–0.6  $\mu\text{m}$  for 850 nm wavelength bands, which makes a grating process easier. The field intensity of the slow-light mode penetrates to the top surface, thus the shallow surface grating offers a strong optical feedback. No regrowth process is needed.

The top view of a fabricated device is shown in Fig. 1 (b). A standard 850 nm VCSEL wafer with 19 pairs top semiconductor DBR is utilized. A wet-oxidation process is carried out to define the active region. The oxide aperture width is 4  $\mu\text{m}$ . The active region length is defined by the length of the top electrode rasing from 300  $\mu\text{m}$  to 500  $\mu\text{m}$ . The surface of the mesa is periodically etched to form lateral Bragg-grating mirrors. While the left-hand side of the cavity is terminated by the oxide region, the right-hand side is coupled to an un-pumped passive waveguide with a length of 2 mm, which works as a low reflectivity end in order to break the dual-mode degeneracy in DFB lasers [30, 31, 32]. Also, this section functions as an amplifier if we inject a current above the threshold, which will be reported elsewhere. The cross-sectional figure of the fabricated surface grating is shown in Fig. 1 (c). The Bragg wavelength is designed at 830 nm, which is near the PL peak wavelength of the VCSEL wafer. The first order grating pitch is 520 nm, which is fabricated by EB lithography followed by dry-etching. 32 nm etching depth is obtained by dry etching process. The first order grating should help in stabilizing the single mode operation of a slow light laser.

### 3. Experimental results and discussions

Figure 2 shows the measured lasing spectra of the fabricated slow light laser with different lengths of 300  $\mu\text{m}$  and 500  $\mu\text{m}$ . Both shows stable single mode operations in the entire current range. As shown in Fig. 2 (a), single-mode slow light lasing at the Bragg wavelength is obtained for the 300  $\mu\text{m}$  long laser until 150 mA with a side mode suppression ratio (SMSR) over 30 dB. Above 150 mA, vertical emission emerges at the wavelength of 858 nm, which causes the saturation of the single slow light mode power. This is due to the thermal induced red shift of the PL wavelength. For a 500  $\mu\text{m}$  laser, the single-mode operation is obtained up to 250 mA with SMSR of 40 dB. Vertical emission can be suppressed through extending the device length to mitigate the self-heating effect as shown in the experimental data. Also, no bonding of the device and no heat-sinking are used for measurements. Thus, higher power operations could be expected with better thermal management. Another method to suppress the vertical emission is to reduce the number of top DBR pair to increase the modal loss for the vertical lasing mode.

The measured light output/current characteristics of the devices are shown in Fig. 3. The photodiode is positioned at a tilted angle to capture only the slow light mode power. Powers from the left side and right side of the device are measured separately. The power discrepancy at two differ-

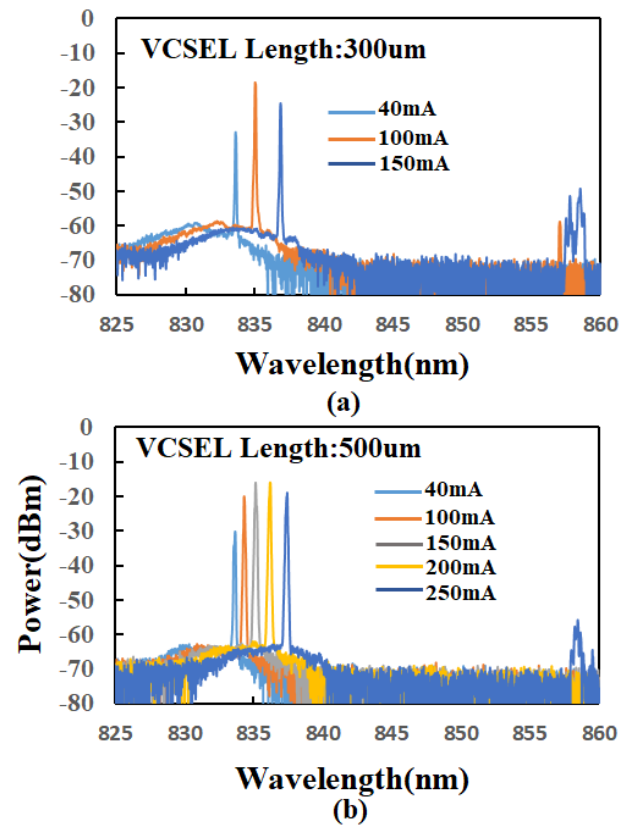


Fig. 2 (a) Measured lasing spectra of (a) a 300  $\mu\text{m}$  long device and (b) a 500  $\mu\text{m}$  long device.

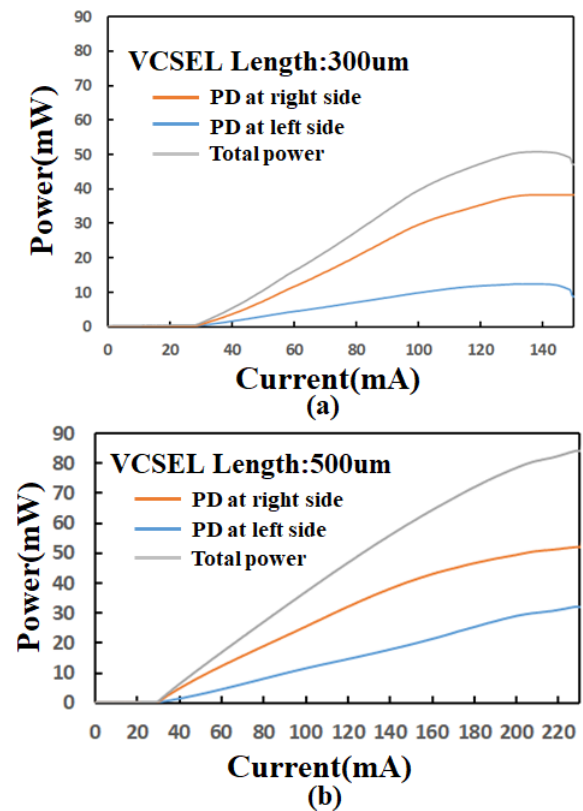
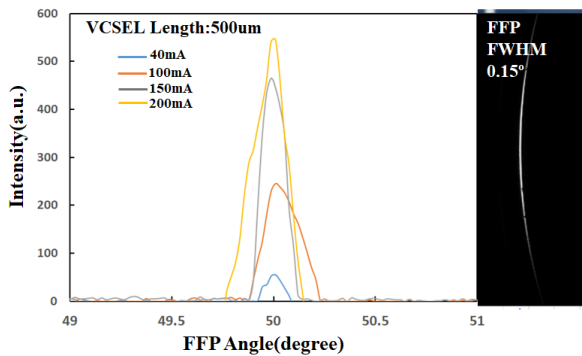


Fig. 3 Measured L/I characteristics of (a) a 300  $\mu\text{m}$  long device and (b) a 500  $\mu\text{m}$  long device



**Fig. 4** Measured FFP under different currents of a 500  $\mu\text{m}$  long slow light laser

ent directions is due to the asymmetric boundary condition at the ends of the slow light laser. The power ratio from different directions is dependent on the device length. It is in agreement with the modeling, which will be reported elsewhere. A total single mode power of 45 mW and 80 mW is obtained for a 300  $\mu\text{m}$  long device and for a 500  $\mu\text{m}$  long device, respectively as shown in Fig. 3. The output power of our slow light laser can be further increased by extending the cavity length since a scaling law has been proven as shown in the figure.

Figure 4 shows the far-field pattern (FFP) of a 500  $\mu\text{m}$  long device from the right side under different currents, the other side shows similar patterns. A single peak at a FFP angle around 50 degree can be seen in the entire current range. The FFP shows a fan-shaped beam according to the rectangular aperture with a diffraction-limited narrow divergence angle of 0.15°. As shown in the figure, the output angle of the slow light from the surface remains stable with different currents. The emission angle of the slow light shows no dependency on the injection currents and hence temperatures because the thermal induced wavelength shift and refractive index change cancels out for the output angle. This characteristic enables our slow light laser to work as a stable light source for various applications such as OCT, LiDAR and so on.

#### 4. Conclusion

In conclusion, we present a slow light laser based on a 1st-order surface grating loaded VCSEL structure. A record single mode power of 80 mW under CW operation is achieved among large oxide aperture VCSELs. Beam divergence as narrow as 0.15° near to the diffraction limit was obtained. The emission angle of the lasing slow-light stays stable with the variation of injection currents. The output power can be further boosted by increasing the device length since the scaling law was proven. Also, a short pulse operation and the thermal management with heat sinking can reduce the self-heating effect for increasing output powers. Further increases in the single mode power toward W-class operation can be expected in the future. Our new single-mode VCSEL with high single mode power and good beam quality can work as a cost-effective and powerful light source for 3D sensing technology.

#### Acknowledgments

This work is partly supported by JST ACCEL.

#### References

- [1] M.A. Taubenblatt: "Optical interconnects for high-performance computing," *J. Lightw. Technol.* **30** (2012) 448 (DOI: [10.1109/JLT.2011.2172989](https://doi.org/10.1109/JLT.2011.2172989)).
- [2] J.A. Tatum, *et al.*: "VCSEL-based interconnects for current and future data centers," *J. Lightw. Technol.* **33** (2015) 727 (DOI: [10.1109/JLT.2014.2370633](https://doi.org/10.1109/JLT.2014.2370633)).
- [3] F. Koyama: "Recent advances of VCSEL photonics," *J. Lightw. Technol.* **24** (2006) 4502 (DOI: [10.1109/JLT.2006.886064](https://doi.org/10.1109/JLT.2006.886064)).
- [4] A. Kasukawa: "VCSEL technology for green optical interconnects," *IEEE Photon. J.* **4** (2012) 642 (DOI: [10.1109/JPHOT.2012.2190723](https://doi.org/10.1109/JPHOT.2012.2190723)).
- [5] A. Larsson: "Advances in VCSELs for communication and sensing," *IEEE J. Sel. Topics Quantum Electron.* **17** (2011) 1552 (DOI: [10.1109/JSTQE.2011.2119469](https://doi.org/10.1109/JSTQE.2011.2119469)).
- [6] T.-H. Tsai, *et al.*: "Ultrahigh speed endoscopic optical coherence tomography using micromotor imaging catheter and VCSEL technology," *Biomedical Optics Express* **4** (2013) 1119 (DOI: [10.1364/BOE.4.001119](https://doi.org/10.1364/BOE.4.001119)).
- [7] C.J. Chang-Hasnain: "Tunable VCSEL," *IEEE J. Sel. Topics Quantum Electron.* **6** (2000) 978 (DOI: [10.1109/2944.902146](https://doi.org/10.1109/2944.902146)).
- [8] E.A. Munro, *et al.*: "Multi-modality optical neural imaging using coherence control of VCSELs," *Optics Express* **19** (2011) 10747 (DOI: [10.1364/OE.19.10747](https://doi.org/10.1364/OE.19.10747)).
- [9] J.-F. Seurin, *et al.*: "High-power vertical-cavity surface-emitting lasers for solid-state laser pumping," *SPIE OPTO* (2012) 827609 (DOI: [10.1117/12.906864](https://doi.org/10.1117/12.906864)).
- [10] H. Moench, *et al.*: "High-power VCSEL systems and applications," *SPIE LASE* (2015) 2076267 (DOI: [10.1117/12.2076267](https://doi.org/10.1117/12.2076267)).
- [11] K. Iga: "Forty years of vertical-cavity surface-emitting laser: invention and innovation," *Jpn. J. Appl. Phys.* **57** (2018) 08PA01 (DOI: [10.7567/JJAP.57.08PA01](https://doi.org/10.7567/JJAP.57.08PA01)).
- [12] V. Jayaraman, *et al.*: "Rapidly swept, ultra-widely-tunable 1060 nm MEMS-VCSELs," *Electron. Lett.* **48** (2012) 1331 (DOI: [10.1049/el.2012.3180](https://doi.org/10.1049/el.2012.3180)).
- [13] M. Okano, *et al.*: "Swept source lidar: simultaneous FMCW ranging and nonmechanical beam steering with a wideband swept source," *Optics Express* **28** (2020) 23898 (DOI: [10.1364/OE.396707](https://doi.org/10.1364/OE.396707)).
- [14] T. Hariyama, *et al.*: "High-accuracy range-sensing system based on FMCW using low-cost VCSEL," *Optics Express* **26** (2018) 9285 (DOI: [10.1364/OE.26.009285](https://doi.org/10.1364/OE.26.009285)).
- [15] B. Chen, *et al.*: "Generation of a high-resolution 3D-printed freeform collimator for VCSEL-based 3D-depth sensing," *Optics Letters* **45** (2020) 5583 (DOI: [10.1364/OL.401160](https://doi.org/10.1364/OL.401160)).
- [16] M. Dummer, *et al.*: "The role of VCSELs in 3D sensing and LiDAR," *SPIE OPTO* (2021) (DOI: [10.1117/12.2577885](https://doi.org/10.1117/12.2577885)).
- [17] M. Miller, *et al.*: "High-power VCSEL arrays for emission in the watt regime at room temperature," *IEEE Photonics Technol. Lett.* **13** (2001) 173 (DOI: [10.1109/68.914311](https://doi.org/10.1109/68.914311)).
- [18] M. Grabherr, *et al.*: "High-power VCSELs: single devices and densely packed 2-D-arrays," *IEEE J. Sel. Topics Quantum Electron.* **5** (1999) 495 (DOI: [10.1109/2944.788411](https://doi.org/10.1109/2944.788411)).
- [19] Z. Wang, *et al.*: "High power and good beam quality of two-dimensional VCSEL array with integrated GaAs microlens array," *Optics Express* **18** (2010) 23900 (DOI: [10.1364/OE.18.023900](https://doi.org/10.1364/OE.18.023900)).
- [20] M. Nakahama, *et al.*: "Slow light VCSEL amplifier for high-resolution beam steering and high-power operations," *CLEO 2016* (2016) 16553630 (DOI: [10.1364/CLEO\\_SI.2016.SF1L.5](https://doi.org/10.1364/CLEO_SI.2016.SF1L.5)).
- [21] Z. Ho, *et al.*: "High power and high beam quality VCSEL amplifier," *ISLC 2018* (2018) 18243082 (DOI: [10.1109/ISLC.2018.8516250](https://doi.org/10.1109/ISLC.2018.8516250)).
- [22] J. Hayakawa, *et al.*: "Watt-class high-power and high-beam-quality VCSEL amplifiers," *SPIE OPTO* (2019) 1093809.
- [23] A. Hassan, *et al.*: "High power and high beam quality surface grating VCSEL," *CLEO* (2021) STh1G.5.
- [24] A.M.A. Hassan, *et al.*: "High-power, quasi-single-mode vertical-

- cavity surface-emitting laser with near-diffraction-limited and low-divergence beam,” *Jpn. J. Appl. Phys.* **59** (2020) 090904 (DOI: [10.35848/1347-4065/ababb6](https://doi.org/10.35848/1347-4065/ababb6)).
- [25] R. Tkach: “Phase noise and linewidth in an InGaAsP DFB laser,” *J. Lightw. Technol.* **4** (1986) 1711 (DOI: [10.1109/JLT.1986.1074677](https://doi.org/10.1109/JLT.1986.1074677)).
- [26] F. Koyama, *et al.*: “1.5-1.6  $\mu\text{m}$  GaInAsP/InP dynamic-single-mode (DSM) lasers with distributed Bragg reflector,” *IEEE J. Quantum Electron.* **19** (1983) 1042 (DOI: [10.1109/JQE.1983.1071967](https://doi.org/10.1109/JQE.1983.1071967)).
- [27] L.M. Miller, *et al.*: “A distributed feedback ridge waveguide quantum well heterostructure laser,” *IEEE Photon. Technol. Lett.* **3** (1991) 6 (DOI: [10.1109/68.68030](https://doi.org/10.1109/68.68030)).
- [28] P. Zhang, *et al.*: “850 nm GaAs/AlGaAs DFB lasers with shallow surface gratings and oxide aperture,” *Optics Express* **27** (2019) 31225 (DOI: [10.1364/OE.27.031225](https://doi.org/10.1364/OE.27.031225)).
- [29] Y. Sakurai and F. Koyama: “Control of group delay and chromatic dispersion in tunable hollow waveguide with highly reflective mirrors,” *Jpn. J. Appl. Phys.* **43** (2004) 5828 (DOI: [10.1143/JJAP.43.5828](https://doi.org/10.1143/JJAP.43.5828)).
- [30] M. Usami, *et al.*: “Asymmetric  $\lambda/4$ -shifted InGaAsP/InP DFB lasers,” *IEEE J. Sel. Topics Quantum Electron.* **23** (1987) 815 (DOI: [10.1109/JQE.1987.1073411](https://doi.org/10.1109/JQE.1987.1073411)).
- [31] K. David, *et al.*: “Basic analysis of AR-coated, partly gain-coupled DFB lasers: the standing wave effect,” *IEEE J. Quantum Electron.* **28** (1992) 427 (DOI: [10.1109/3.123269](https://doi.org/10.1109/3.123269)).
- [32] F. Grillot: “On the effects of an antireflection coating impairment on the sensitivity to optical feedback of AR/HR semiconductor DFB lasers,” *IEEE J. Quantum Electron.* **45** (2009) 720 (DOI: [10.1109/JQE.2009.2013155](https://doi.org/10.1109/JQE.2009.2013155)).